Letter

Entanglement spectrum dynamics as a probe for non-Hermitian bulk-boundary correspondence in systems with periodic boundaries

Pablo Bayona-Pena,[1] Ryo Hanai,[1] Takashi Mori,[2] and Hisao Hayakawa[1]
[1]*Center for Gravitational Physics and Quantum Information, Yukawa Institute for Theoretical Physics, Kyoto University, Kyoto 606-8502, Japan*
[2]*Department of Physics, Keio University, 3-14-1 Hiyoshi, Yokohama 223-8522, Japan*

(Received 26 September 2024; revised 9 March 2025; accepted 17 March 2025; published 7 April 2025)

It has recently been established that open quantum systems may exhibit a strong spectral sensitivity to boundary conditions, known as the non-Hermitian/Liouvillian skin effect (NHSE/LSE), making the topological properties of the system boundary-condition sensitive. In this Letter, we ask the query: Can topological phase transitions of open quantum systems, captured by *open* boundary conditioned invariants, be observed in the dynamics of a system under *periodic* boundary conditions, even in the presence of NHSE/LSE? We affirmatively respond to this question, by considering the quench dynamics of entanglement spectrum in a periodic open quantum fermionic system. We demonstrate that the entanglement spectrum exhibits zero-crossings only when this *periodic* system is quenched from a topologically trivial to nontrivial phase, defined from the spectrum under *open* boundary conditions, even in systems featuring LSE. Our results reveal that non-Hermitian topological phases leave a distinctive imprint on the unconditional dynamics within a subsystem of fermionic systems.

DOI: 10.1103/PhysRevB.111.L140303

Introduction. The recent expansion of phases of matter into the non-Hermitian realm has significantly broadened our understanding of free fermionic systems [1–3]. The presence of non-Hermiticity, which generally arises from the exchange of energy and/or particles of a system with the environment, leads to various exotic phenomena. A paradigmatic example is the emergence of extreme spectral sensitivity to boundary conditions, often referred to as the *non-Hermitian skin effect* (NHSE) [4–24], or *Liouvillian skin effect* (LSE) in the context of open quantum systems [7–12], see also [13,14] for related results in interacting many-body systems. In the presence of NHSE/LSE, the system exhibits exponential localization of eigenstates near its boundaries. This poses a challenge to the conventional understanding of bulk-boundary correspondence: the presence of topological edge states in open boundary conditions (OBC) cannot be inferred from the topological invariant of the Bloch Hamiltonian [5,6]. In this situation, one must extend the conventional Bloch band theory to incorporate complex-valued wave vectors in order to identify topological invariants in OBC [5,6]. This is known as the non-Hermitian bulk-boundary correspondence.

Let us remark, however, a somewhat obvious point that for systems subject to periodic boundary conditions (PBC), the topological transition point is determined by the Bloch Hamiltonian even in the presence of NHSE/LSE. It is tempting to expect that no sign of topological invariants defined from the OBC spectrum can be extracted from the PBC system.

In this Letter, in sharp contrast to this naïve expectation, we show that there are cases where OBC topological invariants can be extracted from the dynamics of the PBC system. This is achieved by examining the quench dynamics of the entanglement spectrum (ES). Initially recognized in the context of a fractional quantum Hall insulator [27] and later formalized for free fermionic [28] and one-dimensional interacting systems [29], the ES has since played a pivotal role in understanding topological phases of both noninteracting and interacting systems. In highly nonequilibrium states, the ES serves as a dynamical probe for wave function topology [30–32]. Recent investigations have partially extended its applicability to non-Hermitian and open quantum systems. In non-Hermitian systems, which effectively describe the dynamics of open systems subject to postselection, it was reported that for point-gapped systems, which exhibit NHSE, ES fails to capture topological properties of the ground state [33]. In open quantum systems, the real line-gap topology was shown to be detectable through the quench dynamics of ES [34–36]. However, these works on open quantum systems, considered systems that do not exhibit LSE [34–36], leaving the effect of boundary conditions sensitivity on the dynamics of ES unclear.

We examine in this Letter an open quantum fermionic lattice exhibiting LSE and show that the dynamics of the ES can serve as a probe for topological phases defined from the OBC spectrum, even when the physical system is in PBC. In particular, we numerically analyze an open quantum model whose dynamics is governed by a dynamical matrix identical to the non-Hermitian Su-Schrieffer-Heeger (SSH) model, a paradigmatic model exhibiting NHSE/LSE [5–7,10,11] and demonstrate that in PBC systems, topological phases defined from the OBC spectrum of Lindbladians are discernible through mode crossings of the ES during quench dynamics. As the ES in open free fermionic systems can be computed from a two-point correlation function of a subsystem [40], our proposal to detect the non-Hermitian bulk-boundary correspondence does not require postselection.

We remark that conventional observables such as the correlation functions and steady-state density profile are *not* generically affected by NHSE/LSE, [9–12,22–24]. Intu-

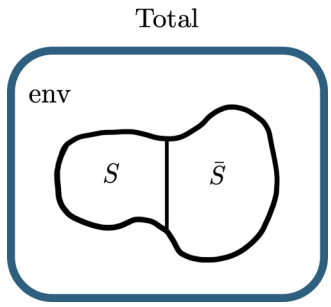

FIG. 1. Illustrati on of tripartition of an open quantum system. The bipartite relevant system $(S + \bar{S})$ is allowed to interact with the environment (env). We focus on the coarse-grained dynamics of the relevant system after tracing out the environmental degrees of freedom $\hat{\rho} = \mathrm{Tr}_{\mathrm{env}}[\hat{\rho}_{\mathrm{tot}}]$.

itively, this is due to the locality of the system: the system's response to an external perturbation applied in the bulk is unaffected by the boundary condition unless the effect reaches the boundary before it dissipates. Our finding here seems to contradict these previous results, but it does not: the ES is a highly nonlocal quantity (for macroscopically large subsystem sizes that we consider in this Letter), making it possible to catch the (nonlocal) spectral sensitivity to boundary conditions stemming from LSE.

The model. We investigate the dynamics of an open quantum system, illustrated in Fig. 1, where a free fermionic system $(S + \bar{S})$ is linearly coupled to a Markovian environment (env). After integrating out the environmental degrees of freedom, the reduced density matrix $\hat{\rho} = \mathrm{Tr}_{\mathrm{env}}\hat{\rho}_{\mathrm{tot}}$ is governed by a quadratic Gorini-Kossakowski-Sudarshan-Lindblad (GKSL) equation [25,26], given by

$$\partial_t \hat{\rho}(t) = -i[\hat{H}, \hat{\rho}(t)] + \sum_{\alpha} \mathcal{D}[\hat{L}_\alpha]\hat{\rho}(t) + \sum_{\alpha} \mathcal{D}[\hat{G}_\alpha]\hat{\rho}(t) = \hat{\mathcal{L}}\hat{\rho}(t), \tag{1}$$

where the superoperator $\hat{\mathcal{L}}$ is the Liouvillian and $\hat{H} = \sum_{i,j=1}^{L} H_{i,j}\hat{c}_i^\dagger \hat{c}_j$ is the Hamiltonian of the relevant system $(S + \bar{S})$. Here, $\hat{c}_i^\dagger$ and $\hat{c}_i$ are creation and annihilation operators of fermions at site i, respectively. The dissipation arising from the coupling of the system to the Markovian reservoir is described by $\mathcal{D}[\hat{M}]\hat{\rho} := \hat{M}\hat{\rho}\hat{M}^\dagger - \frac{1}{2}\{\hat{M}^\dagger\hat{M}, \hat{\rho}(t)\}$. Each coupling to the Markovian reservoir, labeled by α [see Fig. 2(a)], induces incoherent addition or removal of particles and is described by linear jump operators, $\hat{L}_\alpha = \sum_i \ell_i^\alpha \hat{c}_i$ and $\hat{G}_\alpha = \sum_i g_i^{*\alpha}\hat{c}_i^\dagger$, respectively, where ℓ_i^α and g_i^α are complex numbers.

According to the tenfold way classification of quadratic fermionic Lindbladians [38], the entire topology of a quadratic Lindbladian can be characterized by the topological invariants of a non-Hermitian operator $\hat{H}_{\mathrm{eff}}$ [10]:

$$\hat{H}_{\mathrm{eff}} := \hat{H} - \frac{i}{2}(\hat{L} + \hat{G}), \tag{2}$$

where $\hat{L} = \sum_\alpha \hat{L}_\alpha^\dagger \hat{L}_\alpha$, and $\hat{G} = \sum_\alpha \hat{G}_\alpha \hat{G}_\alpha^\dagger$. We note that $\hat{H}_{\mathrm{eff}}$ is different from the conditional Hamiltonian $\hat{H}_{\mathrm{cond}} = \hat{H} - (i/2)(\hat{L} - \hat{G})$ that governs the dynamics of null-jump processes [7,9,10,12,39].

ES crossings as a non-Hermitian bulk-boundary correspondence indicator. To dynamically detect the non-Hermitian bulk-boundary correspondence, we propose examining the ES dynamics after a dissipative quench. As depicted in Fig. 1, we partition the relevant system $(S + \bar{S})$ further into the subsystem $S = \{1, 2, ..., M\}$ and its complement $\bar{S} = \{M + 1, M + 2, ..., L\}$. The reduced density matrix of the subsystem can be written as $\hat{\rho}_S = \mathrm{Tr}_{\bar{S}}\hat{\rho} = (1/Z_S)e^{-\hat{H}_S}$ with $Z_S = \mathrm{Tr}_S[e^{-\hat{H}_S}]$, where $\mathrm{Tr}_{S(\bar{S})}$ denotes the trace over subsystem $S(\bar{S})$. We refer to the spectrum of $\hat{H}_S$ as the ES ϵ_l, the central quantity of interest. Using the property that $\hat{\rho}_S$ is Gaussian, the entanglement Hamiltonian can be decomposed as $\hat{H}_S = \sum_l \epsilon_l \hat{f}_l^\dagger \hat{f}_l$, where $\hat{f}_l$ is a fermionic annihilation operator of the l-th eigenmode. In the absence of the system-environment coupling, this recovers

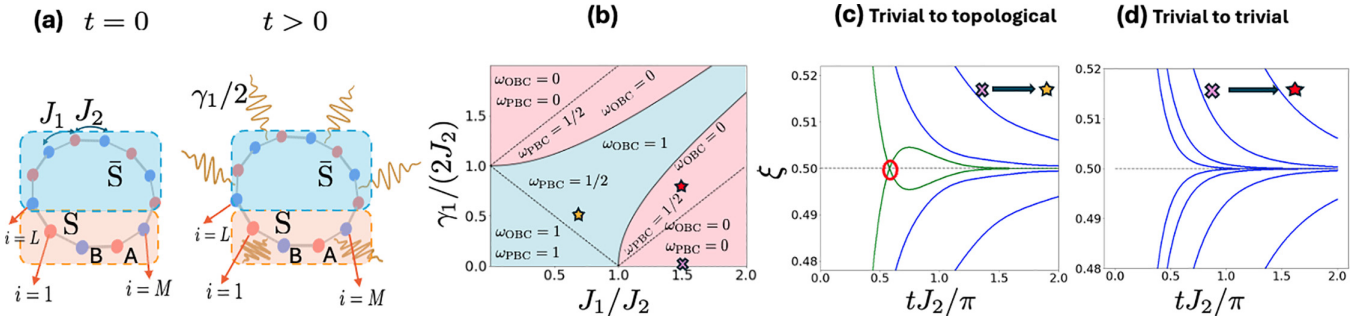

FIG. 2. (a) The system is initially prepared in the trivial ground state of the SSH model [37] under PBC with no dissipation. Then, at $t > 0$, the relevant system $(S + \bar{S})$ is driven out of its initial state by an abrupt change of the hopping parameters J_1, J_2 and a correlated dissipation with rate γ_1 is simultaneously turned on. The relevant system evolves according to the GKLS equation Eq. (1) under PBC. (b) Phase diagram of the Lindbladian SSH model Eq. (7). Topological phase transitions are separated by the solid and dotted lines for OBC and PBC, respectively. (c), (d) ES dynamics for a subsystem S. (c) Trivial to topological quenches for both OBC and PBC spectrum ($\omega_{\mathrm{OBC}} = 1, \omega_{\mathrm{PBC}} = 1/2$) $(J_1/J_2, \gamma_1/(2J_2)) = (0.7, 0.5)$. The green lines represent the four eigenvalues, $\xi_l(t)$, of the covariance matrix $\mathsf{C}_{\mathrm{SS}}(t)$ that are closest to the zero energy entanglement value $\xi = 0.5$ during the time evolution. The other eigenvalues are shown in blue. Four ES eigenvalues cross $\xi = 0.5$ as they decay. (d) Trivial to trivial quenches for OBC spectrum ($\omega_{\mathrm{OBC}} = 0$) $(J_1/J_2, \gamma_1/(2J_2)) = (1.5, 0.8)$ but topological for PBC spectrum ($\omega_{\mathrm{PBC}} = 1/2$). All the eigenvalues, $\xi_l(t)$, of $\mathsf{C}_{\mathrm{SS}}(t)$ are shown in blue. All eigenvalues decay to $\xi = 0.5$ without crossing it. For both cases, we set the initial state to be the (trivial) ground state at $(J_1/J_2, \gamma_1/(2J_2)) = (1.5, 0)$, the system size $L = 20$, and the size of subsystem S is $M = 10$ sites. Note crucially that, while the ES dynamics reflect the OBC spectrum, our physical system is under PBC.

the conventional definition of the ES for closed fermionic systems, which is known to successfully detect bulk-boundary correspondence [27–29].

References [30–32] considered the situation where they first prepared a state corresponding to the ground state of a Hamiltonian in the trivial phase followed by a sudden change in the parameters. They showed that when the postquench Hamiltonian has a topologically nontrivial (trivial) ground state, (no) zero-crossings of the ES occur.

We investigate below a similar setup where we also quench the system from a topologically trivial to a nontrivial or trivial state in an open quantum system governed by Eq. (1) [34–36]. Importantly, the topology of our system is characterized by the non-Hermitian effective Hamiltonian $\hat{H}_{\text{eff}}$, given by Eq. (2), that exhibits NHSE. We find that an analogous phenomenon to the closed-system counterpart occurs, which surprisingly reflects the topology of an *OBC* system even when the system itself is in *PBC*: physically traversing the system is unnecessary to detect topological phases of $\hat{H}_{\text{eff}}$ defined under open boundary conditions.

Practically, in our quadratic system, the ES can be computed from the covariance matrix $\mathsf{C}(t)$, whose (j,i) component is given by the spatial correlation function $[\mathsf{C}]_{j,i}(t) := \text{Tr}_{\text{S}+\bar{\text{S}}}[\hat{\rho}(t)\hat{c}_i^\dagger \hat{c}_j]$ [40]. By taking advantage of the property that the density matrix is always Gaussian (as long as we take the initial state to be Gaussian) and Wick's theorem applies as a result, the ES can be derived from the spectrum of the covariance matrix C_{SS} in the subsystem S defined as the correlation matrix C whose indices are restricted to subsystem S,

$$[\mathsf{C}_{\text{SS}}]_{j,i}(t) := \text{Tr}_{\text{S}+\bar{\text{S}}}[\hat{\rho}(t)\hat{c}_i^\dagger \hat{c}_j];\ (i,j) \in \text{S}, \tag{3}$$

which can be expressed using the reduced density matrix of the subsystem S as $[\mathsf{C}_{\text{SS}}]_{j,i}(t) = \text{Tr}_{\text{S}}[\hat{\rho}_{\text{S}}(t)\hat{c}_i^\dagger \hat{c}_j]$. Letting $\xi_l(t)$ be the eigenspectrum of $\mathsf{C}_{\text{SS}}(t)$, one finds the relation between $\xi_l(t)$ and the ES $\epsilon_l(t)$ [40] (See Supplemental Material (SM) [39]):

$$\xi_l(t) = \frac{1}{e^{\epsilon_l(t)}+1}. \tag{4}$$

An entanglement zero mode with $\epsilon_l = 0$ corresponds to $\xi_l = 0.5$. To investigate the dynamics of ξ_l, we derive from Eq. (1) the following equation for the covariance matrix dynamics [10,12]:

$$i\partial_t \mathsf{C}(t) = \mathsf{H}_{\text{eff}}\mathsf{C}(t) - \mathsf{C}(t)\mathsf{H}_{\text{eff}}^\dagger + i\mathsf{G}, \tag{5}$$

where $[\mathsf{G}]_{i,j} = \sum_\alpha g_i^{*\alpha} g_j^\alpha$ and $[\mathsf{H}_{\text{eff}}]_{i,j} = H_{i,j} - i/2\sum_\alpha(\ell_i^{*\alpha}\ell_j^\alpha + g_i^{*\alpha}g_j^\alpha)$. g_i^α and ℓ_i^α are complex numbers.

Lindbladian SSH model. To be specific, we consider the following system exhibiting LSE [5,11] [Fig. 2(a)]. For the system Hamiltonian, we consider the tight-binding Hamiltonian

$$\hat{H} = \sum_j (J_1 \hat{c}_{A,j}^\dagger \hat{c}_{B,j} + J_2 \hat{c}_{B,j}^\dagger \hat{c}_{A,j+1} + J_3 \hat{c}_{A,j}^\dagger \hat{c}_{B,j+1}) + \text{H.c.} \tag{6}$$

For $J_3 = 0$, the Hamiltonian reduces to the SSH model [37]. The dissipation of our model is given by the following jump operators for $j = 1, 2, \ldots, N$ [see Fig. 2(a)]: $\hat{L}_{j,1} = \sqrt{\frac{\gamma_1}{2}}(\hat{c}_{A,j} + i\hat{c}_{B,j})$, $\hat{G}_{j,1} = \sqrt{\frac{\gamma_1}{2}}(\hat{c}_{A,j}^\dagger - i\hat{c}_{B,j}^\dagger)$, $\hat{L}_{j,2} = \sqrt{\frac{\gamma_2}{2}}(\hat{c}_{B,j} + i\hat{c}_{A,j+1})$, $\hat{G}_{j,2} = \sqrt{\frac{\gamma_2}{2}}(\hat{c}_{B,j}^\dagger - i\hat{c}_{A,j+1}^\dagger)$. Here, we have chosen jump operators such that $\hat{L}_{j,s=1,2}^\dagger = \hat{G}_{j,s=1,2}$, ensuring the system reaches an infinite-temperature state at the long-time limit. The ES asymptotically converges to zero $\epsilon_n = 0$ ($\xi_n = 0.5$), avoiding the ES from crossing zero for trivial reasons with no topological origin [34,41].

This choice of Hamiltonian and jump operators yield the effective Hamiltonian [Eq. (2)],

$$\begin{aligned}\hat{H}_{\text{eff}} = \sum_j [&(J_1 \hat{c}_{A,j}^\dagger \hat{c}_{B,j} + J_2 \hat{c}_{B,j}^\dagger \hat{c}_{A,j+1} \\ &+ J_3 \hat{c}_{A,j}^\dagger \hat{c}_{B,j+1}) + \text{H.c.}] + \sum_j \Big(\frac{\gamma_1}{2}(\hat{c}_{A,j}^\dagger \hat{c}_{B,j} - \hat{c}_{B,j}^\dagger \hat{c}_{A,j}) \\ &+ \frac{\gamma_2}{2}(\hat{c}_{B,j}^\dagger \hat{c}_{A,j+1} - \hat{c}_{A,j+1}^\dagger \hat{c}_{B,j})\Big) - i\frac{\gamma_1+\gamma_2}{2}\hat{n},\end{aligned} \tag{7}$$

with $\hat{n} := \sum_j [\hat{c}_{A,j}^\dagger \hat{c}_{A,j} + \hat{c}_{B,j}^\dagger \hat{c}_{B,j}]$, which is the non-Hermitian SSH model well studied in the literature (except for the constant shift in the imaginary axis that does not affect its topological features) which is known to exhibit NHSE [5,6]. For PBC, the Hamiltonian $\hat{H}_{\text{eff}}$ can be expressed as $\hat{H}_{\text{eff}} = \sum_k \boldsymbol{c}^\dagger(k)\mathsf{H}_{\text{eff}}(k)\boldsymbol{c}(k)$, where $\boldsymbol{c}(k) := (\hat{c}_A(k), \hat{c}_B(k))^T$ with $\hat{c}_{A(B)}(k) = 1/\sqrt{L}\sum_j e^{-ikj}\hat{c}_{A(B),j}$ and $\mathsf{H}_{\text{eff}}(k) = h_1(k)\sigma_x + h_2(k)\sigma_y$, where $h_1(k) = J_1 + (J_2+J_3)\cos(k) - i\gamma_2/2\sin(k)$, $h_2(k) = (J_2 - J_3)\sin(k) + i\gamma_2/2\cos(k) - i\gamma_1/2$. Here, σ_i with $i \in \{x, y, z\}$ are the Pauli matrices and we have ignored the constant shift term. Since the effective Hamiltonian has a sublattice symmetry $\sigma_z \mathsf{H}_{\text{eff}}(k)\sigma_z^{-1} = -\mathsf{H}_{\text{eff}}(k)$, we can define the $\mathbb{Z}$ topological number of $\mathsf{H}_{\text{eff}}(k)$, given by the winding number $\omega_{\text{PBC}} = \oint \frac{dk}{4\pi i}\text{Tr}[\sigma_z \mathsf{H}_{\text{eff}}^{-1}(k)\frac{d}{dk}\mathsf{H}_{\text{eff}}(k)]$ [2]. The winding number can be similarly defined for OBC, ω_{OBC}, by generalizing the momentum integral in the PBC winding number, ω_{PBC}, to those with complex values along the generalized Brillouin zone. (See, e.g., Refs. [6,20] for details.)

First, we focus on the case where $\gamma_2 = 0$, $J_3 = 0$. Here, in PBC, the topological transition point is given by $J_1 = J_2 \pm \gamma_1/2$ or $J_1 = -J_2 \pm \gamma_1/2$ [5]. For OBC, the spectrum can be easily obtained by means of a similarity transformation S, such that H_{eff} and $\bar{\mathsf{H}}_{\text{eff}} := \mathsf{S}^{-1}\mathsf{H}_{\text{eff}}\mathsf{S}$ share the same spectrum. By taking $\mathsf{S} = \text{diag}(1, r, r, r^2, r^2, \ldots, r^{L-1}, r^{L-1}, r^L)$ with $r = \sqrt{|(J_1 - \gamma_1/2)/(J_1 + \gamma_1/2)|}$ [5,6], $\bar{\mathsf{H}}_{\text{eff}}$ becomes the Hermitian SSH model with hopping parameters $\bar{J}_1 = \sqrt{(J_1 - \gamma_1/2)(J_1 + \gamma_1/2)}$ and $\bar{J}_2 = J_2$ provided that $|J_1| > |\gamma_1/2|$. The phase boundary between topological and trivial phases can then be obtained as (assuming $J_1 > 0$ without loss of generality)

$$J_1 = \sqrt{J_2^2 + \left(\frac{\gamma_1}{2}\right)^2} \quad \text{or} \quad \sqrt{-J_2^2 + \left(\frac{\gamma_1}{2}\right)^2}, \tag{8}$$

as shown in Fig. 2(b). The discrepancy between OBC and PBC phase diagrams is due to the NHSE as shown in Fig. 2(b) [2,5,6].

We numerically demonstrate below that the topological transition point in OBC given by Eq. (8) can be detected through the ES dynamics of a PBC system after a quench. In our simulation, we set the prequench state to be the ground

state in the trivial phase of Eq. (7), in the Hermitian limit $\gamma_1 = \gamma_2 = 0$ with $J_3 = 0$.

Figures 2(c) and 2(d) show the quench dynamics of ES for a PBC system. Here, in Fig. 2(c), the post-quench parameters are in the topologically nontrivial phase for both OBC and PBC. In Fig. 2(d), on the other hand, the parameters are chosen such that the post-quench system is in a trivial (nontrivial) phase for a OBC (PBC) system.

For the trivial to topological quench in Fig. 2(c), we observe four ES eigenvalues crossing exactly at the entanglement zero mode energy, $\xi = 0.5$, as they decay. In contrast, in Fig. 2(d), we do not observe any crossings between eigenmodes, which exponentially decay towards the steady state. In the SM [39], we have numerically confirmed that the presence and absence of ES zero-crossings is determined by the phase boundary of the effective Hamiltonian H_{eff} for OBC, given by Eq. (8). This demonstrates a remarkable feature: the ES cares only about the topology of the OBC spectrum. We have also confirmed that the presence (absence) of ES zero-crossings is unaffected by the presence of disorder which respects the symmetries of the effective Hamiltonian $\hat{H}_{\text{eff}}$ and by the strength of uniform on-site balanced gain and loss (that does not affect the topology of $\hat{H}_{\text{eff}}$ but do give rise to a finite lifetime to the response to a local perturbation [9,10,12]), consistent with our expectation that the ES zero-crossings have a topological origin. These findings motivate us to assert that the ES crossings have a topological origin, and their presence (or absence) is determined by the topological invariants of the pre-quench Hamiltonian $\hat{H}$ and the effective Hamiltonian $\hat{H}_{\text{eff}}$.

Finally, we consider the more general case with $\gamma_2 \neq 0$, $J_3 \neq 0$ and demonstrate that the above features remain qualitatively intact even in cases where the effective Hamiltonian H_{eff} cannot be transformed to a Hermitian Hamiltonian. Figure 3(a) shows the single-particle spectrum of the effective Hamiltonian $\hat{H}_{\text{eff}}$ for both OBC and PBC. Similarly to the previous case, we see that the topological transition point, marked by the closing of the energy gap, is different between OBC and PBC, again, due to the NHSE.

Figures 3(b) and 3(c) show the quench dynamics of ES for a PBC system, where, as before, we set the pre-quench state to be the ground state of the Hermitian SSH model in the trivial phase. In Fig. 3(b), the post-quench parameters lie in the topologically nontrivial phase for both OBC ($\omega_{\text{OBC}} = 1$) and PBC ($\omega_{\text{PBC}} = 1/2$), whereas for Fig. 3(c), quench parameters lie in the trivial phase for OBC ($\omega_{\text{OBC}} = 0$) and in the topological phase for PBC ($\omega_{\text{PBC}} = -1/2$). We observe that two pairs of two ES eigenvalues, $\xi_l(t)$, crossing at $\xi = 0.5$ for the trivial to topological quench shown in Fig. 3(b), while Fig. 3(c) shows that no crossings occur for trivial to trivial quenches. This demonstrates that the presence or absence of zero-crossings in the ES dynamics is determined by the OBC phase diagram of the effective Hamiltonian $\hat{H}_{\text{eff}}$. In the SM [39], we have numerically demonstrated that the findings presented in this letter hold true for nonequilibrium quenches, where the system under consideration, $\mathrm{S} + \bar{\mathrm{S}}$, evolves under OBC conditions.

We briefly note that, interestingly, the ES degeneracy at the crossing point observed in the trivial to topological phase quench, which appears in the absence of next-nearest neighbor hopping ($J_3 = 0$) [Fig. 2(c)] and in the Hermitian case [30], is lifted when $J_3 \neq 0$ in our open system scenario. Additionally, we observe that for quenches on open chains, ES crossings remain degenerate. Furthermore, the possibility that ES crossings signal a topological phase transition of the entanglement Hamiltonian, $\hat{H}_{\mathrm{S}} = -\log(Z_{\mathrm{S}}\hat{\rho}_S)$, as reported in the quench dynamics of closed systems [30], remains an open question. We currently lack an explanation for these features, leaving this as a topic for future work.

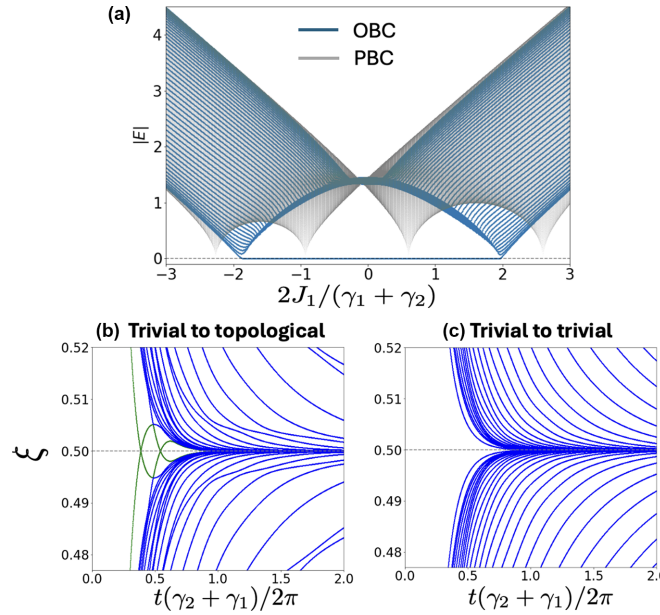

FIG. 3. (a) The blue (gray) lines are the energy bands of the effective Hamiltonian H_{eff} in a finite open chain for $2J_2/(\gamma_1+\gamma_2) = 1.4$, $2J_3/(\gamma_1+\gamma_2) = 1/5$, $2\gamma_1/(\gamma_1+\gamma_2) = 5/3$, $2\gamma_2/(\gamma_1+\gamma_2) = 1/3$ in OBC (PBC). (b),(c) Quench dynamics of ES under PBC. The system is initially prepared in the trivial ground state of the SSH model $(J_2/J_1, J_3/J_1, \gamma_1/J_1, \gamma_2/J_1) = (0, 0, 0, 0)$, with system size $L = 40$, and a subsystem S of $M = 20$ sites. At $t = 0$ the relevant system $(\mathrm{S} + \bar{\mathrm{S}})$ is driven out of equilibrium by an abrupt change in parameters and allowing the system to couple to Markovian reservoirs at a rate $\gamma_i, (i = 1, 2)$. (b) Trivial to topological quench for OBC and PBC spectrum $(2J_1/(\gamma_1+\gamma_2), 2J_2/(\gamma_1+\gamma_2), 2J_3/(\gamma_1+\gamma_2)) = (-1, 1.4, 1/5)$. The green lines represent the four eigenvalues, $\xi_l(t)$, of the covariance matrix $\mathsf{C}_{\mathrm{SS}}(t)$ that are closest to $\xi = 0.5$ during the time evolution. The other eigenvalues are shown in blue. Two pairs of two ES eigenvalues, $\xi_l(t)$, cross $\xi = 0.5$ at different times as they decay. (c) Trivial to trivial (topological) quench for OBC (PBC) spectrum $(2J_1/(\gamma_1+\gamma_2), 2J_2/(\gamma_1+\gamma_2), 2J_3/(\gamma_1+\gamma_2)) = (2.1, 1.4, 1/5)$. All the eigenvalues $\xi_l(t)$ shown in blue decay without zero-crossings.

Conclusions. In summary, our work has revealed th at non-Hermitian bulk-boundary correspondence can be detected through the quench dynamics of the entanglement spectrum, specifically through the presence or absence of zero-crossings. Our results contribute to a deeper understanding of topological phases in open quantum systems.

Acknowledgments. We thank Zongping Gong, Yuto Ashida, Kohei Kawabata, and Tianqi Chen for their helpful discussions. P.B.-P. acknowledges financial support from the Rotary Yoneyama Memorial Scholarship (Masters)

Grant-in-Aid for Scientific Research (B) No. 21H01006. He also thanks RIKEN for their warm hospit ality during his stay there, where part of this work was initiated. R.H. was supported by the Grant-in-Aid for Research Activity Start-up from JSPS in Japan (Grant No. 23K19034). T.M. acknowledges support by JSPS KAKENHI Grant No. JP21H05185 and by JST, PRESTO Grant No. JPMJPR2259. H.H. was supported by the Kyoto University Foundation.

[1] Z. Gong, Y. Ashida, K. Kawabata, K. Takasan, S. Higashikawa, and M. Ueda, Topological phases of non-Hermitian systems, Phys. Rev. X **8**, 031079 (2018).

[2] K. Kawabata, K. Shiozaki, M. Ueda, and M. Sato, Symmetry and topology in non-Hermitian physics, Phys. Rev. X **9**, 041015 (2019).

[3] H. Shen, B. Zhen, and L. Fu, Topological band theory for non-Hermitian Hamiltonians, Phys. Rev. Lett. **120**, 146402 (2018).

[4] V. M. Martinez Alvarez, J. E. Barrios Vargas, and L. E. F. Foa Torres, Non-Hermitian robust edge states in one dimension: Anomalous localization and eigenspace condensation at exceptional points, Phys. Rev. B **97**, 121401(R) (2018).

[5] S. Yao and Z. Wang, Edge states and topological invariants of non-Hermitian systems, Phys. Rev. Lett. **121**, 086803 (2018).

[6] K. Yokomizo and S. Murakami, Non-Bloch band theory of non-Hermitian systems, Phys. Rev. Lett. **123**, 066404 (2019).

[7] F. Song, S. Yao, and Z. Wang, Non-Hermitian skin effect and chiral damping in open quantum systems, Phys. Rev. Lett. **123**, 170401 (2019).

[8] T. Haga, M. Nakagawa, R. Hamazaki, and M. Ueda, Liouvillian skin effect: Slowing down of relaxation processes without gap closing, Phys. Rev. Lett. **127**, 070402 (2021).

[9] G. Lee, A. McDonald, and A. A. Clerk, Anomalously large relaxation times in dissipative lattice models beyond the non-Hermitian skin effect, Phys. Rev. B **108**, 064311 (2023).

[10] A. McDonald, R. Hanai, and A. A. Clerk, Nonequilibrium stationary states of quantum non-Hermitian lattice models, Phys. Rev. B **105**, 064302 (2022).

[11] F. Yang, Q.-D. Jiang, and E. J. Bergholtz, Liouvillian skin effect in an exactly solvable model, Phys. Rev. Res. **4**, 023160 (2022).

[12] S. E. Begg and R. Hanai, Quantum criticality in open quantum spin chains with nonreciprocity, Phys. Rev. Lett. **132**, 120401 (2024).

[13] T. Mori and T. Shirai, Resolving a discrepancy between Liouvillian gap and relaxation time in boundary-dissipated quantum many-body systems, Phys. Rev. Lett. **125**, 230604 (2020).

[14] S. Hamanaka, K. Yamamoto, and T. Yoshida, Interaction-induced Liouvillian skin effect in a fermionic chain with a two-body loss, Phys. Rev. B **108**, 155114 (2023).

[15] N. Okuma, K. Kawabata, K. Shiozaki, and M. Sato, Topological origin of non-Hermitian skin effects, Phys. Rev. Lett. **124**, 086801 (2020).

[16] D. S. Borgnia, A. J. Kruchkov, and R.-J. Slager, Non-Hermitian boundary modes and topology, Phys. Rev. Lett. **124**, 056802 (2020).

[17] K. Imura and Y. Takane, Generalized bulk-boundary correspondence for non-Hermitian topological systems, Phys. Rev. B **100**, 165430 (2019).

[18] L. Xiao, X. Dong, K. Wang, Y. Li, W. Yi, and P. Xue, Non-Hermitian bulk-boundary correspondence in quantum dynamics, Nat. Phys. **16**, 761 (2020).

[19] R. Shen, T. Chen, B. Yang, and C. H. Lee, Observation of the non-Hermitian skin effect and Fermi skin on a digital quantum computer, Nat. Commun. **16**, 1340 (2025)..

[20] Z. Yang, K. Zhang, C. Fang, and J. Hu, Non-Hermitian bulk-boundary correspondence and auxiliary generalized Brillouin zone theory, Phys. Rev. Lett. **125**, 226402 (2020).

[21] G. Lee, T. Jin, Y. X. Wang, A. McDonald, and A. Clerk, Entanglement phase transition due to reciprocity breaking without measurement or postselection, PRX Quantum **5**, 010313 (2024).

[22] S. Longhi, Unraveling the non-Hermitian skin effect in dissipative systems, Phys. Rev. B **102**, 201103 (2020).

[23] N. Okuma and M. Sato, Non-Hermitian skin effects in Hermitian correlated or disordered systems: Quantities sensitive or insensitive to boundary effects and pseudo-quantum-number, Phys. Rev. Lett. **126**, 176601 (2021).

[24] L. Mao, T. Deng, and P. Zhang, Boundary condition independence of non-Hermitian Hamiltonian dynamics, Phys. Rev. B **104**, 125435 (2021).

[25] G. Lindblad, On the generators of quantum dynamical semigroups, Commun. Math. Phys. **48**, 119 (1976).

[26] V. Gorini, A. Kossakowski, and E. C. G. Sudarshan, Completely positive dynamical semigroups of N-level systems, J. Math. Phys. **17**, 821 (1976).

[27] H. Li and F. D. M. Haldane, Entanglement spectrum as a generalization of entanglement entropy: Identification of topological order in non-Abelian fractional quantum Hall effect states, Phys. Rev. Lett. **101**, 010504 (2008).

[28] L. Fidkowski, Entanglement spectrum of topological insulators and superconductors, Phys. Rev. Lett. **104**, 130502 (2010).

[29] F. Pollmann, A. M. Turner, E. Berg, and M. Oshikawa, Entanglement spectrum of a topological phase in one dimension, Phys. Rev. B **81**, 064439 (2010).

[30] Z. Gong and M. Ueda, Topological entanglement-spectrum crossing in quench dynamics, Phys. Rev. Lett. **121**, 250601 (2018).

[31] C. Wang, P. Zhang, X. Chen, J. Yu, and H. Zhai, Scheme to measure the topological number of a Chern insulator from quench dynamics, Phys. Rev. Lett. **118**, 185701 (2017).

[32] M. McGinley and N. R. Cooper, Topology of one-dimensional quantum systems out of equilibrium, Phys. Rev. Lett. **121**, 090401 (2018).

[33] L. Herviou, N. Regnault, and J. H. Bardarson, Entanglement spectrum and symmetries in non-Hermitian fermionic non-interacting models, SciPost Phys. **7**, 069 (2019).

[34] S. Sayyad, J. Yu, A. G. Grushin, and L. M. Sieberer, Entanglement spectrum crossings reveal non-Hermitian dynamical topology, Phys. Rev. Res. **3**, 033022 (2021).

[35] E. Starchl and L. M. Sieberer, Relaxation to a parity-time symmetric generalized Gibbs ensemble after a quantum quench in a driven-dissipative Kitaev chain, Phys. Rev. Lett. **129**, 220602 (2022).

[36] E. Starchl and L. M. Sieberer, Quantum quenches in driven-dissipative quadratic fermionic systems with parity-time symmetry, Phys. Rev. Res. **6**, 013016 (2024).

[37] W. P. Su, J. R. Schrieffer, and A. J. Heeger, Solitons in polyacetylene, Phys. Rev. Lett. **42**, 1698 (1979).

[38] S. Lieu, M. McGinley, and N. R. Cooper, Tenfold way for quadratic Lindbladians, Phys. Rev. Lett. **124**, 040401 (2020).

[39] See Supplemental Material at http://link.aps.org/supplemental/10.1103/PhysRevB.111.L140303 for a detailed explanation of the distinction between conditional and unconditional dynamics in open quantum systems, explicit derivation of entanglement spectrum (ES) for closed systems, along with additional numerical evidence supporting the topological origin of ES crossings.

[40] I. Peschel, Calculation of reduced density matrices from correlation functions, J. Phys. A **36**, L205 (2003).

[41] For example, consider a system which has loss only (i.e., $\hat{G}_{j,s=1,2} = 0$) with the initial state given by an all-occupied state. In this case, the system keeps losing particles from the system and would eventually converge to a vacuum state. This situation gives rise to the ES crossing for a trivial reason: the ES at the initial state $\xi_l(t = 0) = 1$ converge to $\xi_l(t \to \infty) = 0$, which gives rise to ES crossing $\xi_l(t) = 0.5$ at finite time t, irrespective of the topology of $\hat{H}_{\text{eff}}$.